# International Journal of Engineering

# The Transient Dynamics of a Beam Mounted on Spring Supports and Equipped with the Nonlinear Energy Sink

S. Mahmoudkhani*

*Aerospace Engineering Department, Faculty of New Technologies and Engineering, Shahid Beheshti University, Tehran, Iran*

| *P A P E R  I N F O* | *A B S T R A C T* |
|---|---|
| | The transient dynamics of a beam mounted on springer-damper support and equipped with a nonlinear energy sink (NES) is investigated under the effects of shock loads. The equations of motion are derived using the Hamilton's principle leading to four hybrid ordinary and partial differential equations and descritized using the Galerkin method. An adaptive Newmark method is employed for accurate and efficient numerical simulation and the results are used to assess the efficiency of the NES by conducting various parametric studies. The mechanisms of targeted energy transfer from the beam to the NES are indicated using the wavelet transform and Hilbert–Huang transform of the responses. Numerous modes are recognized to contribute to the response and the modes with smaller particiaption of the rigid-body motions are found to be strongly engaged in the transient resonance capture (TRC) at the initial stage of the motion. The modes with dominant rigid-body motions are, however found to be less engaed in an effective TRC. The enhanced empirical mode decomposition, with different masking signals are used to extract narrow-band intrinsic mode functions (IMFs) and simultaneous 1:1 transient resonances are observed between different IMFs of the responses especially at the initial stage of the motion.<br><br>*doi*: 10.5829/ije.2017.30.10a.16 |

## NOMENCLATURE

| | | | |
|---|---|---|---|
| $m$ | Mass per unit length of the beam | $k_1, k_2, \bar{k}_1, \bar{k}_2$ | The physical and nondimensional stiffnesses of the edge spring supports |
| $L$ | Length of the beam | $c_1, c_2, \bar{c}_1, \bar{c}_2$ | The physical and nondimensional damping coefficients of the edge support |
| $M$ | Total mass of the beam and the NES | $c_s, \bar{c}_s$ | The physical and nondimensional damping coefficients of the NES |
| $M_s, \bar{m}_s$ | The physical and nondimensional masses of the NES | $\theta$ | The rigid-body rotation of the beam |
| $E$ | Elasticity modulus | $w, \bar{w}$ | The physical and nondimnsional elastic defelction of the beam |
| $I_{Ayy}$ | The second moment of area | $E_{NES}$ | The proportion of the external energy input dissipated by the damper of the NES |
| $I_{Myy}$ | The mass moment of inertia of the beam about the mass center | $D(t)$ | The ratio of the instantaneous total energy in the NES to the total energy of the system |
| $\alpha, \bar{\alpha}$ | The physical and nondimensional coefficients of the cubic stiffness of the NES | | |

## 1. INTRODUCTION

Flexible beams mounted on spring supports can be considered as a simplified model of many engineering structures such as car chasses and axles, fluid-conveying

*Corresponding Author's Email: s_mahmoudkhani@sbu.ac.ir (S. Mahmoudkhani)*

pipes and many flexible components with isolator mounts. Due to the flexibility of the support in these structures, the beam may be displaced with both rigid body motions and elastic deformations. Thus the rigid and elastic modes of the beam would be simultaneously excited under transient and dynamic loadings, leading to multi-frequency response with large distances between the frequencies. If the vibration mitigation is required

for these structures, as is the case in many engineering applications, the adopted method must be wide-band. The method should also be robust to system parameter changes, since in most applications the environmental condition changes the system properties. The dynamic vibration absorber which may be thought as one of the appropriate methods [1, 2], cannot be effectively used for these applications since it is highly sensitive to system parameters and should be tuned to a specific frequency. The Nonlinear Energy Sink (NES) may be a better tool in these situations since it does not have linear preferential frequencies and thus is able to engage in nonlinear resonance with any modes of the linear system [3]. The NES has also been shown to be robust and perform with high efficiency in relatively large ranges of system parameters. The concept of NES is rather new and is not yet entered in industrial applications. On the other hand, theoretical and experimental studies are ongoing to demonstrate their effectiveness for use in engineering structures. In this regard, continuous systems are particularly considered as they are widely used for modeling the engineering structures. The work of Georgiades and Vakakis [4] is one of the first published studies in this area that investigated the targeted energy transfer (TET) from a simply-supported beam to a locally attached NES. The capability of the NES to alleviate the effects of shock was explored in this study. The nonlinear dynamics of a rod with single and multi DOF NES was further investigated in a series of studies [5, 6]. The multi-frequency transitions were recognized in these studies using the frequency-energy plot (FEP) of the periodic orbits of the Hamiltonian system and the Wavelet Transform (WT) of the damped response, superimposed to the FEPs. The Empirical Mode Decomposition (EMD) method accompanied by the Hilbert transforms (The so-called Hilbert–Huang transform, (HHT)) were also implemented and proved to be a powerful method for system identification and determination of resonance captures in systems with damped strongly nonlinear absorbers. The WT and HHT are both signal processing tools that are able to identify the variation of the frequency components of non-stationary signals with time and thus are best suited for transient dynamical analyses [7]. The WT expands signals in terms of windowed certain basis functions and provides higher time and frequency resolution by decreasing the interval of window function for higher frequencies [8]. The HHT does not need any priori-defined functional basis and extracts the intrinsic mode functions (IMFs) of signals based on an adaptive empirical basis [9]. The Hilbert transform is then used to determine the amplitude and phase of the IMFs. For most dominant IMFs, the computed amplitudes and phases correspond to the slow-flow dynamics of the system [8, 9]. Therefore, combination of WT and HHT seems to

provide a powerful tool for studying the strongly nonlinear dynamics of the system. This tool was also used in other studies by Georgiades and Vakakis [10] for analysis of plates with the NES. Some other studies that investigted the effects of the NES on the vibration of engineering structures are performed by Ahmadabadi and Khadem [11] for vibration control of cantilever beams, and by Parseh et al. [12] and Kani et al. [13] for vibration analysis of linear and nonlinear beams. The effect of the NES on the aeroelastic behavior of the wing model was also investigated by Ebrahimzade et al. [14]. The vibration mitigation of a continuous rotor-blisk-journal bearing using the NES was also investigated by Bab et al. [15].

The present study aims to study the efficiency and influence of the NES on transient dynamics of a beam mounted on spring-damper supports. For this purpose, the kinematics of the elastic system is first determined based on arbitrarily large rigid-body motions. The equations of motion (EOM) are then obtained by omitting the nonlinear terms corresponding to rigid-body motion, assuming that the beam motion remains small during the vibration. The result is a set of four coupled partial differential equations for the rigid-body rotational and translational and elastic motions of the beam, and transverse motion of the NES. The equations are then discretized by the Galerkin's method and solved by an adaptive Newmark method. The WT is implemented together with the HHT to carefully track the nonlinear resonance interactions occurring during the TET from the primary system to the NES. To extract the IMFs of responses, which contain numerous frequency components, the EDM procedure is used in the present study with different masking signals for different IMFs of the response. The results also include comprehensive parametric studies, which determine the appropriate values of NES parameters and its location to achieve high efficiencies.

## 2. FORMULATION

In Figure 1 the geometry of the problem including a flexible beam mounted on spring-dampers at its edges is displayed, where $m$, $L$ and $EI$ represent the mass per unit length, the length and the rigidity of the beam, respectively. The attached NES is also shown in the figure by a mass, $m_s$ together with a viscose damper with the damping coefficient $c_s$ and an essentially nonlinear spring with $\alpha$ being the coefficient of the cubic stiffness of the spring.

The inertial and body-fixed frames, which are used for describing the motion of the beam are presented in Figure 2.
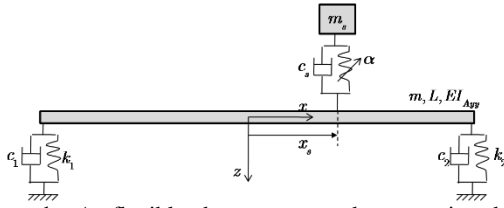
**Figure 1.** A flexible beam mounted on spring-damper supports with the NES attached to an arbitrary point
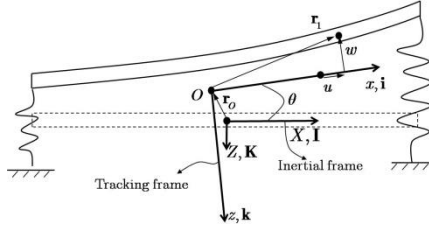


**Figure 2.** The inertial and tracking coordinate systems used for analysis

The orientation and attachment point of the body-fixed frame (The so-called tracking frame) are, however, unknown since the beam undergoes coupled rigid and elastic motion. The general way to deal with this problem is to impose proper constraint on the tracking frame [16]. Appropriate and common constraints are that the origin of the tracking frame must always be on the mass center of the beam and the elastic deflection be orthogonal to the rigid body modes [16]. The origin of the tracking frame would be always on the mass center if the following equation is satisfied:

$$\int_L \mathbf{r}_1(x,t)mdx = 0, \tag{1}$$

where $m$ is the constant mass per unit length. Also, according to Figure 2, $\mathbf{r}_1$ is defined as:

$$\mathbf{r}_1 = w(x,t)\mathbf{k} + [x + u(x,t)]\mathbf{i}, \tag{2}$$

where $w(x,t)$ and $u(x,t)$ represent the axial and transverse displacements of the beam. The orthogonality of $w(x,t)$ and $u(x,t)$ to rigid–body modes (translational and rotational motions) can also be imposed by the following equations:

$$\int_L w(x,t)mdx = 0, \int_L xw(x,t)mdx = 0,$$
$$\int_L u(x,t)mdx = 0, \tag{3}$$

Equation (1) will be reduced to the following form by using Equations (2) 0and (3):

$$\int_L xmdx = 0, \tag{4}$$

which implies that the origin always coincides with the mass center of the undeformed body.

Considering Figure 2, the total displacement vector, $\mathbf{r}$, of any point of the beam can be defined by $\mathbf{r} = \mathbf{r}_O + \mathbf{r}_1$ where $\mathbf{r}_O = W_r(t)\mathbf{K} + U_r(t)\mathbf{I}$. Taking the derivative of $\mathbf{r}$ with respect to time, $t$, the velocity vector can be obtained as:

$$\mathbf{v} = \dot{\mathbf{r}}_O + \dot{u}(x,t)\mathbf{i} + \dot{w}(x,t)\mathbf{k} + (\dot{\theta}\mathbf{j}) \times \mathbf{r}_1 =$$
$$\dot{W}_r(t)\mathbf{K} + \dot{U}_r(t)\mathbf{I} +$$
$$\left[\dot{w}(x,t) - \dot{\theta}(t)x - \dot{\theta}(t)u(x,t)\right]\mathbf{k} +$$
$$\left[\dot{u}(x,t) + \dot{\theta}(t)w(x,t)\right]\mathbf{i}. \tag{5}$$

where the overscript, dot, means differentiation with respect to time. The formulations presented until now for the kinematics of the system are in their general form, where no assumptions are imposed on the magnitudes of different displacement components introduced above. However, in the following, the horizontal and axial displacements, $U_r$ and $u$ are assumed to be negligible relative to the transverse and vertical displacements and so are dropped. Moreover, since only the linear vibration of the suspended beam is considered in present analysis, $w$, $W_r$ and also $\theta$ are assumed to be small. By these assumptions, the relations, $\sin(\theta) = \theta$ and $\cos(\theta) = 1$ can be employed, which leads to the conclusion that $W_r$ would be equal to $w_r$. Therefore, in the remaining analyses, only three infinitesimal displacements, $w$, $W_r$ and $\theta$ will be used for describing the beam's motion.

For derivation of EOM, the Hamilton's principle is used, which requires that:

$$\int_{t_1}^{t_2} \left(\delta T - \delta U + \delta W_f\right)dt = 0, \tag{6}$$

where $\delta$ is the variational operator, $T$ is the kinetic energy, $U$ is the strain energy and $W_f$ is the work done by external forces. For $T$ the corresponding expression is as follows:

$$T = \frac{1}{2}\int_L \left\{m\mathbf{v}^T\mathbf{v} + m_s\left[\dot{w}_s - \dot{w}(x_s) - \dot{w}_r\right]^2\right\}dx. \tag{7}$$

Introducing Equations (3), (4) and (5) into (7) and taking the variation of the ensuing result, would give $\delta T$ in terms of the displacement and rotation of the beam.

The variation of strain energy ($\delta U$) arisen from the small deformations of elastic components (i.e., beam and springs) can also be defined as follows:

$$\delta U = \int_{-\frac{L}{2}}^{\frac{L}{2}} \left\{EI_{Ayy}\left(\frac{\partial^2 w}{\partial x^2}\right)\left(\frac{\partial^2 \delta w}{\partial x^2}\right) + \right.$$
$$\sum_{i=1,2} k_i \chi(x,x_i)\delta\chi(x,x_i,t)\Delta(x-x_i) +$$
$$\left. \alpha\left(\chi(x,x_s,t) - w_s\right)^3 \left(\delta\chi(x,x_i,t) - \delta w_s\right)\Delta(x-x_s)\right\}dx, \tag{8}$$

where $\chi(x, x_i, t) = w_r + w(x) - x_i\theta$, and $\Delta$ is the Dirac delta function, $x_1 = -L/2$, $x_2 = L/2$ and $x_s$ denotes the $x$-coordinate of the NES attachment point. Next $\delta W_f$ is expressed as:

$$\delta W_f = \int_L \left\{ f(x,t)\left(\delta w_r + \delta w - x\delta\theta\right) - \right.$$
$$\sum_{i=1,2} c_i \dot\chi(x, x_i, t)\delta\chi(x, x_i, t)\Delta(x - x_i) - \tag{9}$$
$$\left. c_s\left(\dot\chi(x, x_s, t) - \dot w_s\right)\left(\delta\chi(x, x_i, t) - \delta w_s\right)\Delta(x - x_s)\right\} dx,$$

where $f(x,t)$ is the force per unit length acting on the beam, which is assumed to be in the form of concentrated loads applied at the edges of the beam. Hence $f(x,t)$ is defined by: $f(x,t) = \Delta(x - x_1)F_1(t) + \Delta(x - x_2)F_2(t)$. Substituting Equations (7)-(9) into 0 and employing the extended fundamental lemma of the calculus of variation, the hybrid EOMs including the ordinary and partitial differentioal equations can be obtained. The Galerkin method [17, 18] is then applied using the expansion $w = \sum_{j=1}^{N} \eta_j(t)\phi_j(x)$, to obtain the following discritized equations of motion:

$$I_{Myy}\ddot\theta - \left[\alpha\left(\chi(x, x_s, t) - w_s\right)^3 + c_s\left(\dot\chi(x, x_s, t) - \dot w_s\right)\right]x_s -$$
$$\sum_{i=1,2} k_i\left(\chi(x, x_i, t) + c_i\dot\chi(x, x_i, t)\right)x_i = -F_1(t)x_1 - F_2(t)x_2,$$

$$M\ddot w_r + \sum_{i=1,2} k_i\chi(x, x_i, t) + c_i\dot\chi(x, x_i, t) +$$
$$c_s\left(\chi(x, x_s, t) - \dot w_s\right) + \alpha\left(\chi(x, x_s, t) - w_s\right)^3 =$$
$$F_1(t) + F_2(t),$$

$$M_s\ddot w_s - \alpha\left(\chi(x, x_s, t) - w_s\right)^3 \tag{10}$$
$$-c_s\left(\dot\chi(x, x_s, t) - \dot w_s\right) = 0,$$

$$\hat a_i\ddot\eta_i + \hat a_i\omega_i^2\eta_i + m_1\phi_i(x_m)\sum_{j=1}^{N}\ddot\eta_j\phi_j(x_m) +$$
$$\alpha\left(\chi(x, x_s, t) - w_s\right)^3\phi_i(x_s) +$$
$$c_s\left(\dot\chi(x, x_s, t) - \dot w_s\right)\phi_i(x_s) +$$
$$\sum_{i=1,2}\left(k_i\chi(x, x_i, t) + c_i\dot\chi(x, x_i, t)\right)\phi_i(x_i)$$
$$= F_1(t)\phi_i(x_1) + F_2(t)\phi_i(x_2),$$

where $\phi_i$, corresponds to the linear elastic modes of the free-free beam. In Equation (10), $\hat a_i = \int_0^L m\phi_i^2 dx$, and $I_{Myy}$ is the mass moment of inertia of the beam about the mass center.

Equation (10) represents $3 + N$ nonlinear ordinary differential equations that can be presented in the following matrix form:

$$\mathbf{M}\ddot{\mathbf{q}} + \mathbf{g}(\mathbf{q}, \dot{\mathbf{q}}) - \mathbf{f}(t) = 0, \tag{11}$$

where $\mathbf{q} = \{\theta, w_r, w_s, \eta_1, ..., \eta_N\}^T$, $\mathbf{M}$ is the mass matrix, $\mathbf{g}(\mathbf{q}, \dot{\mathbf{q}})$ is a nonlinear vector function of $\mathbf{q}$ and $\dot{\mathbf{q}}$, and $\mathbf{f}$ is the vector of external forces in Equation (10). These equations can be solved by the Newmark method. It must be noted that due to the highly nonlinear behavior and moderately large degrees of the system, the time steps of the numerical simulation should be carefully chosen by repeating the simulation with different time steps to achieve convergent results. To avoid this, an adaptive time-stepping is incorporated in the Newmark method, using the procedure proposed in the literature [19]. The solution is then used to determine the efficacy of the NES by calculating the proportion of the external energy input dissipated by the damper of the NES as follows [4]:

$$E_{NES} = \lim_{t \to \infty} \frac{c_s\int_0^t\left[\dot w(x_s) + \dot w_r - x_s\dot\theta - \dot w_s\right]^2}{\int_0^t\sum_{i=1,2} F_i(t)\left[\dot w(x_i) + \dot w_r - x_i\dot\theta\right]dt}, \tag{12}$$

To indicate the mechanism of energy transfer between the NES and the beam, the ratio of the instantaneous total energy in the NES to the total energy of the system ($D(t)$) is also computed using the relation $D(t) = SE_{NES} / SE_{total}$ where [4]:

$$SE_{NES} = \frac{1}{2}m_s\dot w_s^2 + \frac{1}{4}\alpha\left[w(x_s) + w_r - x_s\theta - w_s\right]^4,$$
$$SE_{total} = SE_{NES} +$$
$$\frac{1}{2}\sum_{i=1,2} k_i\left[w(x_i) + w_r - x_i\theta\right]^2 + \frac{1}{2}m\dot w_r^2 + \frac{1}{2}I_{Myy}\dot\theta^2 + \tag{13}$$
$$\frac{1}{2}m_s\dot w_s^2 + \frac{1}{2}EI_{Ayy}\int_{x_1}^{x_2} w''^2 dx + \frac{1}{2}\int_{x_1}^{x_2} m\dot w^2 dx.$$

By plotting $D(t)$ versus time, the rate and mechanism of the energy transfer in different regimes of the motion can be identified.

## 3. NUMERICAL RESULTS

The numerical studies are performed in this section using the following non-dimensional parameters:

$$\bar k_i = \frac{L^3}{EI_{Ayy}}k_i, \ \ \bar c_i = c_i\sqrt{\frac{L^2}{EI_{Ayy}m}}, \ (i = 1, 2, s),$$
$$\bar\alpha = \frac{L^5}{EI_{Ayy}}\alpha, \bar m_s = \frac{M_s}{M}, \bar w = \frac{w}{L}, \bar w_r = \frac{w_r}{L}, \tag{14}$$
$$\bar t = \sqrt{\frac{EI_{Ayy}}{mL^4}}t, \bar\omega = \sqrt{\frac{mL^4}{EI_{Ayy}}}\omega, \bar A_i = \frac{A_iL^2}{EI_{Ayy}}, i = 1, 2.$$

The geometric and material properties of the beam used in the numerical analysis are:

$$E = 70\,\text{GPa}, L=1, m=2.7\,\text{kg/m},$$
$$I_{Myy} = 0.225\,\text{kg.m}^2, I_{Ayy} = 3.34 \times 10^{-8}\,\text{m}^4 \tag{15}$$

The nondimensional stiffness and damping parameters of the supports are also taken as $\bar{k}_1 = \bar{k}_2 = 150$ and $\bar{c}_1 = \bar{c}_2 = .02$ in all the analyses unless otherwise stated. Moreover, the exciation forces are assumed to be of half-sine shock, which are defined as:

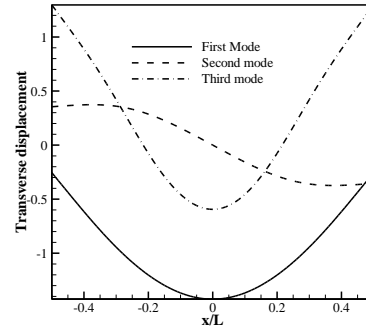$$F_i = A_i \sin(\frac{2\pi}{T_1}t)H(\frac{T_i}{2}-t), i = 1, 2, \tag{16}$$

where $H$ is the heaviside unit step function. To check the validity of the present formulation, the time response of the middle point of the beam is computed and compared by Ansys (Not presented here due to the limited space).

The non-dimensional frequencies calculated for the system without NES are given in Table 1. The first two frequencies in this table correspond to the modes with dominant rigid-body motions although the elastic deformation is also presented in these modes. This is illustrated in Figure 3 which displays the first six linear mode shapes of the linear beam on spring supports. It is evident that the first and third modes have similar shapes except that the first mode includes the translational rigid-body motion. The linear damped frequencies of the beam with the NES are also obtained in Table 2 for different attachment points and $\bar{c}_s = 0.1$ and $\bar{m}_s = 0.04$. Comparing the results with Table 1, the linear frequencies and especially the first mode frequecny are seen to be mostly influenced when the NES is attached to the midpoint of the beam. However, the changes are not considerable since the NES has not a linear spring.
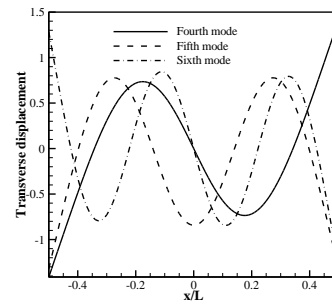
In the above and the following analyses, seven numbers of trial function are used which is found to give convergent results. The sensitivity of the NES efficiency ($E_{NES}$) to different system parameters are investigated in contour plots of Figurse 4-6. Variation of $E_{NES}$ with the nonlinear spring coefficient ($\bar{\alpha}$) and the attachment point of the NES ($x_s$) is depicted in Figure 4. The result shows a considerable influence of the attachment point on the efficiency of the beam, which is considerably higher than the influence of $\bar{\alpha}$.



(a)



(b)

**Figure 3.** First six linear modes of the beam without NES mounted on spring supports.

**TABLE 2.** Non-dimensional natural frequencies of the beam with NES mounted on spring supports

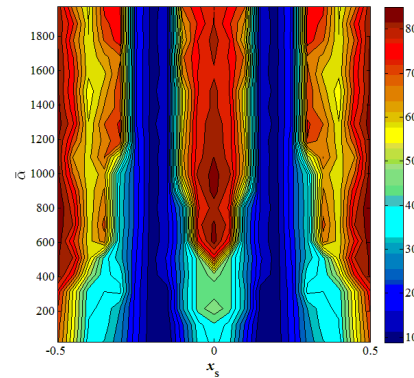| Mode no. | 1 | 2 | 3 | 4 | 5 |
|---|---|---|---|---|---|
| $x_s = -0.5$ | 8.73 | 25.20 | 42.15 | 71.99 | 126.17 |
| $x_s = -0.3$ | 8.71 | 25.20 | 42.17 | 72.01 | 126.18 |
| $x_s = 0$ | 8.67 | 25.20 | 42.18 | 72.01 | 126.18 |



**Figure 4.** Variation of the NSE efficiency with $\bar{\alpha}$ and the NES attachment point ($x_s$) when $\bar{A}_1 = \bar{A}_2 = 70, \bar{T}_1 = \bar{T}_2 = .07$
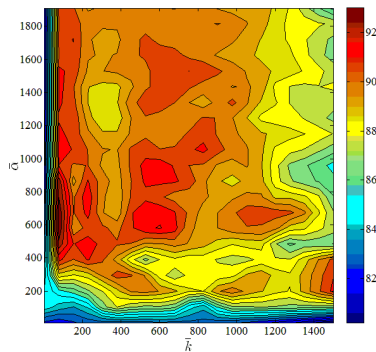
**TABLE 1.** Non-dimensional natural frequencies of the beam without NES mounted on spring supports

| Mode no. | 1 | 2 | 3 | 4 | 5 | 6 |
|---|---|---|---|---|---|---|
| $\bar{\omega}$ | 8.74 | 25.20 | 42.12 | 72.01 | 126.16 | 202.98 |

**Figure 5.** Variation of the NSE efficiency with $\bar{\alpha}$ and support stiffness when $\bar{k}_1 = \bar{k}_1 = \bar{k}, \bar{A}_1 = \bar{A}_2 = 0.5\bar{k}, \bar{T}_1 = \bar{T}_2 = 0.1(2\pi / \bar{\omega}_1)$
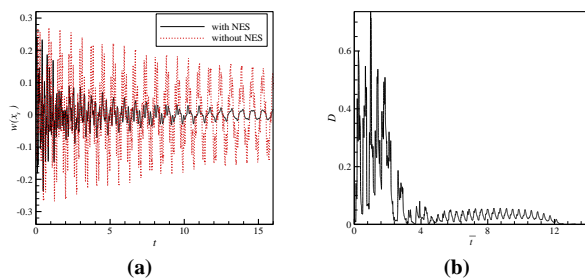


**Figure 6.** (a) The beam response and (b) the instantaneous percentage of the total energy in the NES

The efficiency is expectedly much higher in regions near the mid-point and edges of the beam. This implies that the beam response has higher amplitudes at these points as is the case in the first and third modes of the beam. Hence it can be deduced that the contribution of the first and third modes to the response may be dominant. Detailed analysis to determine the dominant modes of the response is performed in the next subsection. Also, for the beam with NES attached to the midpoint, efficiencies of higher than 60% are attainable for $\bar{\alpha}$ greater than 500. The sensitivity of the efficiency to $\bar{\alpha}$ is however lower when the NES is attached to the edges of the beam.

The second parametric study is performed to determine the effect of the support stiffness on the performance of the NES with different values of $\bar{\alpha}$. The support stiffness would in fact affect the distribution of the natural frequencies of the system. In fact, when the support stiffness is sufficiently low, the lower modes with dominant rigid-body motions have much smaller frequencies than the dominantly elastic modes. Hence, this parametric study may also illustrate the sensitivity of the NES performance to the frequency distribution of the system. The result is presented in Figure 5, which is obtained by assuming $\bar{A}_1, \bar{A}_2, T_1,$ and

$T_2$ are varied with $\bar{k}_1$ and $\bar{k}_2$ such that $\bar{A}_1 = \bar{A}_2 = 0.5\bar{k}_1$ and $T_1 = T_2 = 0.1(2\pi / \bar{\omega}_1)$. Figure 5 shows a non-smooth variation of the efficiency with $\bar{k}_1$ and $\bar{\alpha}$, which is mostly the result of highly nonlinear behavior of the system. Moreover, the regions with lower support stiffness show lower efficiency. This is more pronounced at lower values of $\bar{\alpha}$, but as $\bar{\alpha}$ increases, the region with poor NES performances becomes narrower. This observation may imply that the NES with lower values of $\bar{\alpha}$ would not act properly when the frequency ratios between elastic and almost rigid-body modes of the system are high.

The dynamics of the elastically supported beam equipped with the NES, is studied first, by calculating the beam response at the attachment point and also by calculating the instantaneous percentage of the total energy in the NES. The results are given in Figure 6 for the parameter values, $\bar{A}_1 = \bar{A}_2 = 70$, $\bar{m}_s = 0.04$, $\bar{\alpha} = 570$ and $\bar{c}_s = 0.1$. In 0Figure 6(a) the response of the beam without the NES is also included to illustrate the effect of the NES in mitigating the beam response. The time evolution of the TET from the primary system to the NES is illustrated in Figure 6(b), which shows that the beam energy at the initial stage of oscillations is considerably transferred, in almost irreversible manner, to the NES. As the nondimensional time approaches 2, the total energy of the NES is completely dissipated or transferred back to the beam. After time 2, another regime of the motion, accompanied by another almost irreversible energy transfer, appears. The percentage of the NES total energy is however much lower than the initial stage of the motion. The existence of two regimes of motion is also evident in Figure 6(a), which implies that the dominant frequencies of the oscillation and thus the modes contributing to the response are different in these two regimes.

To better understand the mechanism of the energy transfer and the modes involved in the observed regimes of the motion, the WT of the difference between the NES response and the beam attachment point response (i.e., $\bar{w}(-0.5) - \bar{w}_s$) is depicted in Figure 7. To compute the WT, the built-in function of Matlab ("cwft"), which uses the FFT algorithm is used with the complex Morlet wavelet. It is found that the FFT-based WT gives more accurate results. Moreover, since the response signals contained different largely spaced frequencies, the use of a single center frequency for the Morlet WT may not give accurate results. Hence, the frequency spectrum of the response is first computed using the FFT method and then divided into smaller bands. The WT is then separately computed for each band with its own center frequency.

The horizontal lines in Figure 7 and also other figures that include WT results, represent the linear

frequency of the structure without NES. According to this figure, the high energy transfer observed in the first regime of the response can be attributed to the occurrence of the transient resonance capture (TRC) by two modes whose frequencies are far from the linear frequencies of the structure. This indicates the presence of the strong nonlinearity in the response, which means that the motion is localized to the NES. The frequencies of these two strongly nonlinear modes are between the second and fourth linear modes of the structures. A weaker contribution of the modes with frequencies near the fourth and fifth linear modes of the structure can also be seen in the initial stage of the oscillation. The first two linear modes of the system that contain dominant rigid body motions have not been engaged in resonance at the first regime of the motion. As time increases beyond the end of the first regime (i.e., $\bar{t} = 2$), another resonance capture is observed near the first linear mode. Hence it is expected that the NES has smaller oscillation amplitude in this regime as confirmed by Figure 6(b).

Further studies on the dynamics of the response are performed by extracting the IMFs of the response. The time evolution of the frequency components of the response may be better illustrated by this method. It must be noted that the time histories obtained for the nonlinear transient response of the beam and the NES have some closely spaced frequency components. Moreover some higher frequency components with smaller amplitudes exist in the signals. In such a case, the standard EMD method may not be able to extract the monocomponent or narrowband IMFs [8]. One way of dealing with this problem is to use the masking signals [8, 9]. In the present study, different masking signals of the form, $x_{mask} = x_m \sin(v_m t)$ are used in the EMD procedure for extracting each IMF, where $x_m$ and $v_m$ are given in Table 3. To obtain these values, a try and error process is performed requiring that the computed IMFs are sufficiently orthogonal and narrowband.
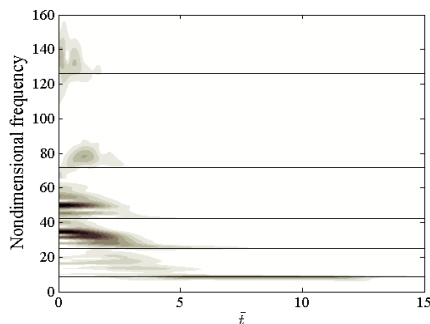
**TABLE 3.** The parameter values of the masking signals of $x_{mask} = x_m \sin(v_m t)$ used in the EMD method to extract the IMFs of (a) the beam response and (b) the NES response

| (a) | | | | |
|---|---|---|---|---|
| | **IMF #1** | **IMF #2** | **IMF #3** | **IMF #4** | **IMF #5** |
| $x_m$ | .075 | 0.175 | 0.125 | 0.1 | 0.125 |
| $v_m$ | 150 | 70 | 50 | 40 | 25 |

| (b) | | |
|---|---|---|
| | **IMF #1** | **IMF #2** | **IMF #3** |
| $x_m$ | .42 | 0.12 | 0.3 |
| $v_m$ | 60 | 35 | 22 |

The orthogonality of the IMFs is checked by calculating the overall index of orthogonality introduced elsewhere [8]. Better orthogonality between the modes may be achieved if this index is sufficiently small. Moreover to eliminate the numerical end effects due to the Gibbs phenomenon, the signals are expanded by adding their mirror image using the method described in the literature [8].

The dominant IMFs of the beam and NES obtained for the case with the NES attached to the edge are presented in Figure 8. The completeness of the extracted IMFs is also verified (not presentd here) by comparing the reconstructed signal with the original one. The reconstructed signal is obtained from the extracted IMFs using the method described in the literature [8].

Figure 8 shows that the highest order IMFs of the beam and NES (i.e., sixth IMF of the beam and fourth IMF of the NES), which correspond to the lowest frequency modes, have lower decaying rates than the other IMFs and thus present in both regimes of the motion identified in Figure 6. The fourth IMF of the NES has specially gained the highest participation in the second regime ($\bar{t} > 2$) of the response as its amplitude had begun to increase in this regime. This behavior indicates the transfer of the energy from lower order IMFs of the NES to the fourth modes and is especially responsible for decrease of the NES efficiency at the second regime of the motion.

To identify the IMFs that are captured in resonance, the corresponding instantaneous frequencies are presented in Figure 9 together with WT of the NES and the beam response at the edge. In this figure the IMFs of the NES and beam with nearly equal frequencies are given next to each other to display the occurrence of 1:1 resonance interaction between these IMFs. The figure shows that at the first regime of the motion, the second IMF of the NES engages in resonance with the fourth IMF of the beam. This interaction is mainly resposible for the dissipation of the energy since the amplitudes of these IMFs have the greatest amplitudes at the first regime of the motion.
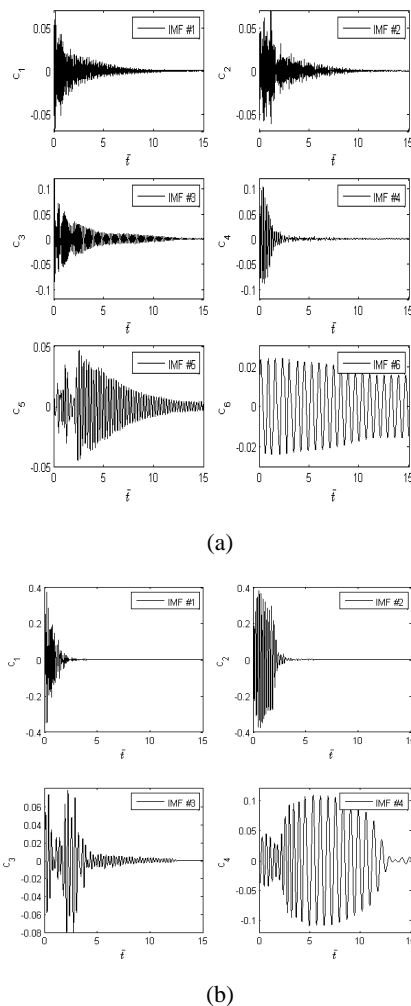


**Figure 7.** The WT of the difference between the response of NES and the beam at the attachment point (a) when the NES is attached to the edge

(a)



(b)

**Figure 8.** The dominant IMFs of (a) the beam response at the edge and (b) the NES response
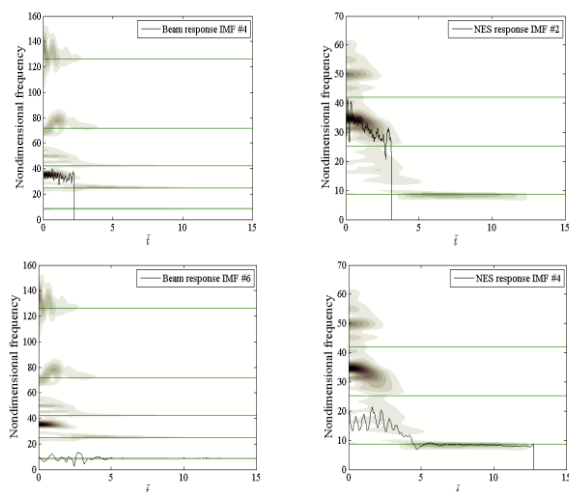


**Figure 9.** The instantaneous frequencies of different IMFs of the response accompanied with WT for the beam edge (left column) and the NES (right column)

At the second regime, the 1:1 interaction occurs between the fourth IMF of the NES and sixth IMF of the beam as seen at the last row of Figure 9. These IMFs correspond to a weakly nonlinear mode near the first linear mode of the beam. It must be noted that some spikes that appeared in the frequencies of the IMFs in Figure 9 are due to elimination of the frequencies with low modulation amplitudes. These frequencies are in fact set to zero in the present study to give a better view of the frequencies of dominant IMFs in the response.

## 4. CONCLUSION

The influence of the locally attached NES on the transient dynamics of a beam mounted on springs was investigated using the WT and HHT signal processing tools. The governing equations of motion were derived by separating the motion into the rigid body and elastic displacements. Numerical simulations were performed by an adaptive Newmark method and the results were used to assess the performance of the NES. The effects of different NES parameters on its efficiency were examined. It was found that the efficiency is highly dependent on the attachment point and best results can be obtained for the case with the NES attached to the edges. The vibration of the system with considerably low support stiffness was also found to be less attunated by the NES. The dynamics of the system and the mechanism of the observed TET were also studied by the time-frequency analysis of the responses using the WT and HHT. Due to the contribution of different-frequency modes to the response, the EDM was employed using different masking signals to extract each IMFs of the responses. The results showed the occurrence of the TRC by different strongly nonlinear modes of the system at initial stage of the motion. Corresponding frequencies of these modes were above the second linear modes of the structure, implying that the interaction occurs between modes with dominant elastic deformations. However, at later stage of the motion, the TRC occurred near the first, dominantly rigid-body mode of the beam. The energy transfer was not, however, considerable in this regime of motion. Simultaneous 1:1 transient resonances between different IMFs of the NES and the beam responses were also observed in both regimes of the motion.

## 5. REFERENCES

1.   Pourzeynali, S. and Esteki, S., "Optimization of the tmd parameters to suppress the vertical vibrations of suspension bridges subjected to earthquake excitations", *Iranian International Journal of Engineering, IJE Transaction B (Application)*, Vol. 22, No. 1, (2009), 23-34.

2.   Saberi, L. and Nahvi, H., "Vibration analysis of a nonlinear system with a nonlinear absorber under the primary and super-harmonic resonances", *International Journal of Engineering-Transactions C: Aspects*,  Vol. 27, No. 3, (2013), 499-507.

3.   Lee, Y., Vakakis, A.F., Bergman, L., McFarland, D., Kerschen, G., Nucera, F., Tsakirtzis, S. and Panagopoulos, P., "Passive non-linear targeted energy transfer and its applications to vibration absorption: A review", *Proceedings of the Institution of Mechanical Engineers, Part K: Journal of Multi-body Dynamics*,  Vol. 222, No. 2, (2008), 77-134.

4.   Georgiades, F. and Vakakis, A., "Dynamics of a linear beam with an attached local nonlinear energy sink", *Communications in Nonlinear Science and Numerical Simulation*,  Vol. 12, No. 5, (2007), 643-651.

5.   Tsakirtzis, S., Lee, Y., Vakakis, A., Bergman, L. and McFarland, D., "Modelling of nonlinear modal interactions in the transient dynamics of an elastic rod with an essentially nonlinear attachment", *Communications in Nonlinear Science and Numerical Simulation*,  Vol. 15, No. 9, (2010), 2617-2633.

6.   Tsakirtzis, S., Vakakis, A.F. and Panagopoulos, P., "Broadband energy exchanges between a dissipative elastic rod and a multi-degree-of-freedom dissipative essentially non-linear attachment", *International Journal of Non-Linear Mechanics*,  Vol. 42, No. 1, (2007), 36-57.

7.   Besanjideh, M. and Mahani, M.F., "Nonlinear and non-stationary vibration analysis for mechanical fault detection by using emd-fft method", *International Journal of Engineering-Transactions C: Aspects*,  Vol. 25, No. 4, (2012), 363-372.

8.   Lee, Y.S., Tsakirtzis, S., Vakakis, A.F., Bergman, L.A. and McFarland, D.M., "Physics-based foundation for empirical mode decomposition", *AIAA journal*,  Vol. 47, No. 12, (2009), 2938-2963.

9.   Kerschen, G., Vakakis, A.F., Lee, Y., McFarland, D. and Bergman, L., "Toward a fundamental understanding of the hilbert-huang transform in nonlinear structural dynamics", *Journal of Vibration and Control*,  Vol. 14, No. 1-2, (2008), 77-105.

10.  Georgiades, F. and Vakakis, A.F., "Passive targeted energy transfers and strong modal interactions in the dynamics of a thin plate with strongly nonlinear attachments", *International Journal of Solids and Structures*,  Vol. 46, No. 11, (2009), 2330-2353.

11.  Ahmadabadi, Z.N. and Khadem, S., "Nonlinear vibration control of a cantilever beam by a nonlinear energy sink", *Mechanism and Machine Theory*,  Vol. 50, (2012), 134-149.

12.  Parseh, M., Dardel, M., Ghasemi, M.H. and Pashaei, M.H., "Steady state dynamics of a non-linear beam coupled to a non-linear energy sink", *International Journal of Non-Linear Mechanics*,  Vol. 79, (2016), 48-65.

13.  Kani, M., Khadem, S., Pashaei, M. and Dardel, M., "Vibration control of a nonlinear beam with a nonlinear energy sink", *Nonlinear Dynamics*,  Vol. 83, No. 1-2, (2016), 1-22.

14.  Ebrahimzade, N., Dardel, M. and Shafaghat, R., "Performance comparison of linear and nonlinear vibration absorbers in aeroelastic characteristics of a wing model", *Nonlinear Dynamics*,  Vol. 86, No. 2, (2016), 1075-1094.

15.  Bab, S., Khadem, S., Shahgholi, M. and Abbasi, A., "Vibration attenuation of a continuous rotor-blisk-journal bearing system employing smooth nonlinear energy sinks", *Mechanical Systems and Signal Processing*,  Vol. 84, (2017), 128-157.

16.  Baruh, H., "Analytical dynamics, WCB/McGraw-Hill Boston, (1999).

17.  Heydari, H., Ghazavi, M., Najafi, A. and Rahmanian, S., "Nonlinear dynamics of the rotational slender axially moving string with simply supported conditions", *International Journal of Engineering-Transactions C: Aspects*,  Vol. 29, No. 6, (2016), 834-841.

18.  Abdollahi, D., Ivaz, K. and Shabani, R., "A numerical improvement in analyzing the dynamic characteristics of an electrostatically actuated micro-beam in fluid loading with free boundary approach", *International Journal of Engineering-Transactions A: Basics*,  Vol. 29, No. 7, (2016), 1005-114.

19.  Zeng, L.F., Wiberg, N.E., Li, X. and Xie, Y., "A posteriori local error estimation and adaptive time-stepping for newmark integration in dynamic analysis", *Earthquake Engineering & Structural Dynamics*,  Vol. 21, No. 7, (1992), 555-571.

# The Transient Dynamics of a Beam Mounted on Spring Supports and Equipped with the Nonlinear Energy Sink

S. Mahmoudkhani

*Aerospace Engineering Department, Faculty of New Technologies and Engineering, Shahid Beheshti University, Tehran, Iran*

| *P A P E R   I N F O* | چکیده |
|---|---|
| | دینامیک گذرای تیر با تکیه‌گاه‌های فنری و مجهز به جاذب غیرخطی ارتعاش، تحت اثر بار شوک اعمالی مورد بررسی قرار گرفت. معادلات حاکم با استفاده از اصل همیلتون استخراج شد که منجر به چهار معادله دیفرانسیلی شامل معادلات معمولی و جزئی مربوط به مودهای صلب تیر، حرکت جاذب غیرخطی و و تغییرشکل الاستیک تیر شد. روش گالرکین نیز برای گسسته‌سازی معادلات و دستیابی به معادلات زمانی مورد استفاده قرارگرفت. برای حل عددی از روش حل نیومارک با امکان تنظیم اتوماتیک گام استفاده شده و برای بررسی کارایی جاذب از طریق مطالعه پارامتریک به‌کارگرفته شد. چگونگی انتقال هدفمند انرژی از تیر به جاذب نیز با استفاده از اعمال تبدیل ویولت و تبدیل هیلبرت-هوانگ به پاسخ زمانی مورد مطالعه قرار گرفت. مطالعات نشان دهنده حضور مودهای متعدد در پاسخ و درگیر شدن  قابل توجه مودهای با سهم پایین از حرکت صلب تیر در پدیده تشدید گذرا در زمان‌های ابتدایی حرکت بود که منجر به میرایی قابل توجه انرژی در تیر می‌شد. در مقابل، مودهای با سهم بیشتر از حرکت صلب به میزان کمتری درگیر با تشدید گذرا شدند. از روش تجزیه مود تجربی در کنار سیگنال‌های ماسک مختلف نیز برای استخراج توابع مود ذاتی استفاده شده، و تشدید ۱:۱ بین مودهای ذاتی حاضر در پاسخ، به‌ویژه در زمان‌های ابتدایی مشاهده شد.

***doi**: 10.5829/ije.2017.30.10a.16* |